# OH OBSERVATIONS IN THE DIRECTIONS OF GALACTIC THERMAL SOURCES

By R. X. McGee,* F. F. Gardner,* and B. J. Robinson*

[*Manuscript received April* 14, 1967]

*Summary*

A survey for the hydroxyl line radiation has been made in the directions of 30 radio sources (most of them thermal) with the 210 ft telescope of beamwidth $12'\cdot 2$ and the multichannel line receiver of bandwidths 10 and 37 kHz. The line at frequency 1665·401 MHz was observed for all sources and the other three lines at 1612, 1667, and 1720 MHz were observed for 10 of the more important sources. The latter were investigated for circular and linear polarization.

Twenty-six sources showed absorption lines in their directions, many at two or more radial velocities. Apparent opacities ranged from 0·4 to less than 0·002.

Fourteen sources showed emission lines. In general, the emission was strongly circularly polarized.

Linear polarization was low except for a value of 45% in one source.

An attempt was made to locate the OH clouds in space with the aid of a model of galactic rotation. OH gas appeared to be spread throughout the spiral arms of hydrogen. The ratio of OH to HI was less in the outer arms than towards the centre source Sagittarius A but it varied somewhat randomly in the inner arms. There is little doubt that OH emission and in many cases OH absorption occur close to HII regions.

## I. Introduction

Observations of the distribution of the interstellar hydroxyl radical have been mainly confined to the directions of radio sources. Absorption was originally detected at the OH-line frequencies in the spectrum of a few strong continuum sources. Later, anomalous line emission of high intensity was found for a number of thermal sources close to the galactic plane. No thermal emission from OH which would allow a general distribution of the molecule to be mapped has been seen. Reviews of earlier work have been given elsewhere (Robinson 1967; Robinson and McGee 1967).

Previous OH observations for a number of HII regions have been described by McGee *et al.* (1965) and Dieter, Weaver, and Williams (1966). In the present investigation we have made observations at the OH frequencies on about 30 of the stronger thermal sources within the declination range of the Parkes radio-telescope (i.e. south of Dec. +27°). The OH line at 1665·401 MHz was used for all sources and the other three lines at 1612, 1667, and 1720 MHz for about one-third of them. Most of the latter sources were also checked for linear and circular polarization at 1665 MHz.

* Division of Radiophysics, CSIRO, University Grounds, Chippendale, N.S.W.

TABLE 1

POSITIONS AND PHYSICAL CHARACTERISTICS OF OH CLOUDS

| (1) Source | (2) Position (1950·0) R.A. h m s | (2) Dec. ° ′ | (3) Galactic Coordinates $l^{II}$ ° | (3) $b^{II}$ ° | (4) $T_c$ (°K) | (5) R.V. (km/sec) | (6) $T_L$ (°K) | (7) R.M.S. Noise (°K) | (8) Apparent Opacity | (9) Half-width (km/sec) | (10) Line Freq. (MHz) | (11) R.V. Excited H (km/sec) | (12) R.V. HI (km/sec) | (13) Distance (kpc) |
|---|---|---|---|---|---|---|---|---|---|---|---|---|---|---|
| Crab nebula (i) | 05 31 29 | +21 59·4 | 184·5 | −5·8 | 600 | — | — | 0·8 | <0·002 | — | 1665 | — | +4, +10·5A | 1·1(opt.) |
| | | | | | | | | 1·0 | <0·002 | — | 1667 | | | |
| Orion nebula (ii) | 05 32 47 | −05 24·7 | 209·0 | −19·4 | 205 | +8 | 4E | 0·3 | — | 36 | 1665 | 0 | +8·5E, +2A | 0·5(opt.) |
| | | | | | | +2·7 | 7E | Narrow peaks | — | ~2·7 | | | | |
| | | | | | | +7·1 | | | | | | | | |
| | | | | | | +21·0 | | | | | | | | |
| 30 Doradus | 05 38 57 | −69 07·3 | 279·5 | −31·7 | 25 | — | — | 1·2 | <0·08 | — | 1665 | — | +278E | 52(opt.) |
| RCW 38 (iii) | 08 57 18 | −47 19·7 | 267·9 | −1·1 | 100 | +1·3 | 8·5A | 0·9 | 0·085 | 6·0 | 1665 | | — | 0·5 |
| | | | | | | +2·9 | 10A | 0·8 | 0·1 | 6·5 | 1667 | +4 | | |
| RCW 36 | 08 57 34 | −43 32·2 | 265·1 | +1·5 | 17 | +10·9 | 3·4A | 0·8 | 0·2 | 4·0 | 1665 | | | 1·5 |
| | | | | | | +27 | 5·4E | 0·9 | — | 2·0 | 1665 | | | 3·5 |
| RCW 46 | 10 04 55 | −56 56·4 | 282·0 | −1·2 | 24 | −7·5 | 2·4A | 1·4 | 0·1 | 3·2 | 1665 | | | |
| | | | | | | 0 | 2·7 E | 1·4 | | 1·7 | 1665 | | | 4, kinematic distance unreliable |
| | | | | | | +3·4 | 6·5 E | | — | 2·2 | | | | |
| | | | | | | +6·8 | 3·4 E | | | 2·2 | | | | |
| RCW 49 | 10 22 27 | −57 31·1 | 284·3 | −0·3 | 115 | −20 | 1·0A | (0·3) | 0·01 | (12) | 1665 | | | No kin. dist. compatible with −20, but see η-Carinae |
| η-Carinae | 10 42 12 | −59 22·6 | 287·5 | −0·64 | 105 | −21 | 2·0A | (0·2) | 0·02 | (4) | 1667 | −20, −24 | | 1·6(opt.) |
| | | | | | | — | Nil | 0·4 | <0·05 | — | 1665 | | | |
| RCW 57 | 11 13 15 | −60 58·5 | 291·6 | −0·5 | 110 | −8·2 | 2·7A | 0·8 | 0·02 | 2·5 | 1665 | −12 | | 1 |
| 1207–62 | 12 07 23 | −62 30·8 | 298·2 | −0·3 | 26 | +3·6 | 5·8A | 1·4 | 0·22 | 2·4 | 1665 | | −52 to +116E, −25 to +25A | 9·5, no kinematic distance compatible |
| | | | | | | −52 | 1·4A | (0·6) | 0·05 | (11) | 1665 | | | |
| 1308–62 (iv) | 13 08 38 | −62 20·1 | 305·3 | +0·2 | 55 | −36·3 | 12·0E | 0·8 | — | 4·8 | 1665 | −31 | −67 to +115E, −53 to +3A | 3 or 8·5 See Section IV |
| | | | | | | −38·5 | 4·8A | 1·2 | 0·09 | 2·0 | 1667 | | | |
| | | | | | | −43·6 | 3·4A | | 0·06 | 3·0 | | | | |
| 1404–61 | 14 04 06 | −61 09·6 | 311·9 | +0·1 | 12 | −7·7 | 3·5E | 1·4 | — | 2·9 | 1665 | | | 12·5 |

| | | | | | | | | | | | | | | |
|---|---|---|---|---|---|---|---|---|---|---|---|---|---|---|
| 1437–59 | 14 37 33 | −59 48·1 | 316·3 | −0·02 | 9 | −4·0 | 3·6A | 1·4 | 0·40 | 2·0 | 1665 | | | |
| | | | | | | −9·0 | 2·0A | | 0·22 | 3·5 | | | | 14 |
| 1441–59 | 14 41 38 | −59 36·6 | 316·8 | −0·05 | 29 | −36·7 | 3·7A | 1·1 | 0·13 | 3·0 | 1665 | | | 2·5(or 12) |
| | | | | | | −25·6 | 4·8A | | 0·16 | 2·6 | | | | 1·5(or 13) |
| 1442–59 | 14 42 05 | −59 12·1 | 317·0 | +0·3 | 13 | −19·4 | 3·2A | 1·4 | 0·25 | 2·4 | 1665 | | | 13·5(or 1·5) |
| 1541–53 | 15 41 04 | −53 58·1 | 326·7 | +0·56 | 35 | −31·1 | 3·1A | 1·4 | 0·09 | 2·8 | 1665 | | −105 to +80E, | 2(or 14·5) |
| | | | | | | −15·2 | 5·1E | | — | 2·3 | | | −90 to +20A | 15·5(or 1) |
| 1548–56 | 15 48 31 | −56 03·3 | 326·2 | −1·74 | 29 | −12·6 | 1·4A | (0·5) | 0·05 | (10) | 1665 | | −100 to +90E, | No kinematic distance |
| | (Nonthermal shell source, ∼30′ diam.) | | | | | −91 | 1·0A | | 0·03 | (15) | | | −100 to +25A | 8·5 |
| | | | | | | −42 | 1·0A | | 0·03 | (11) | | | | 3(or 11·5) |
| 1548–54 | 15 48 57 | −54 26·3 | 327·3 | −0·52 | 34 | −94 | 1·0A | (0·4) | 0·03 | (14) | 1665 | | −155 to +75E, | 8 |
| | | | | | | −54·0 | 5·1A | 1·4 | 0·15 | 2·3 | 1665 | | −75 to +20A | 3·5(or 13) |
| | | | | | | −50·6 | 3·4A | | 0·10 | 3·5 | | | | 3·5(or 13) |
| | | | | | | −42·9 | 3·7A | | 0·11 | 6·5 | | | | 3(or 13·5) |
| | | | | | | −25·5 | 4·1A | | 0·12 | 2·8 | | | | 2(or 15) |
| 1608–51 (v) | 16 08 14 | −51 18·4 | 331·5 | −0·05 | 26 | −100·5 | 4·1A | 1·0 | 0·16 | 2·0 | 1665 | | 150 to +85E, | 10(or 7) |
| | | | | | | −97·1 | 5·3A | | 0·20 | 2·5 | | | | |
| | 16 08 39 | −51 21·3 | | | | −90·3 | 17·6E | 0·8 | — | 4·0 | 1665 | −87 | −150 to −20A | 11(or 6·5) |
| 1617–50 (vi) | 16 17 06 | −50 31·0 | 332·2 | −0·4 | 49 | −59·0 | 5·0A | 0·8 | 0·10 | 4·0 | 1665 | | | 4 |
| | | | | | | −45·0 | 3·2A | | 0·07 | 2·0 | | | | 3 |
| | 16 17 16 | −50 27·6 | | | | −54·8 | 2·6E | 0·8 | — | 2·7 | 1665 | −49 | | 4 |
| | | | | | | −51·6 | 14·7E | | — | 2·5 | | | | |
| | 16 17 41 | −50 28·8 | | | | −59 | 2·0E | 1·4 | — | 3·6 | 1667 | | | |
| | | | | | | −46·4 | 2·7A | | 0·06 | 2·5 | | | | |
| 1618–49 | 16 18 16 | −49 57·8 | 333·6 | −0·2 | 49 | −114·5 | 1·4A | (0·5) | 0·03 | (20) | 1665 | −113 | | |
| | | | | | | −73·0 | 1·0A | | 0·02 | (6) | | −69 | | 2·5 |
| | | | | | | −55·0 | 1·4A | | 0·03 | (5) | | −50 | | 2 |
| | | | | | | −31·4 | 1·4E | | — | (7) | | | | |
| | | | | | | −22·0 | 1·7A | | 0·03 | (10) | | | | |
| | | | | | | +8·0 | 3·2A | 1·4 | 0·07 | 2·8 | 1665 | | | |
| 1630–47 | 16 30 52 | −47 30·1 | 336·8 | +0·05 | 38 | −120 | 1·7A | (0·5) | 0·04 | (11) | 1665 | | −140 to > +150 E,A | 7·5 |
| | | | | | | −53·2 | 5·4A | 1·4 | 0·14 | 2·2 | 1665 | | | 4 |
| 1636–46 | 16 36 59 | −46 17·2 | 338·4 | +0·1 | 37 | −92 | 1·3A | (0·5) | 0·04 | (20) | 1665 | | | 7(or 11·5) |
| | | | | | | −24 | 1·4A | | 0·04 | (23) | | | | 2 |
| 1716–38 | 17 16 35 | −38 54·1 | 348·7 | −1·02 | 32 | +30·6 | 4·8A | 1·4 | 0·15 | 2·0 | 1665 | | | Within "inner zone" |

TABLE 1 (*Continued*)

| (1) Source | (2) Position (1950·0) R.A. h m s | Dec. ° ′ | (3) Galactic Coordinates $l^{II}$ ° | $b^{II}$ ° | (4) $T_c$ (°K) | (5) R.V. (km/sec) | (6) $T_L$ (°K) | (7) R.M.S. Noise (°K) | (8) Apparent Opacity | (9) Half-width (km/sec) | (10) Line Freq. (MHz) | (11) R.V. Excited H (km/sec) | (12) R.V. HI (km/sec) | (13) Distance (kpc) |
|---|---|---|---|---|---|---|---|---|---|---|---|---|---|---|
| NGC 6334 (vii) | 17 17 02 | −35 47·0 | 351·3 | +0·7 | 68 | −4·5 | 6·8A | 0·8 | 0·10 | 4·3 | 1665 | −4 | | 0·6 |
| | | | | | | +5·5 | 3·4A | | 0·05 | 3·5 | | | | No kinematic |
| | | | | | | | | (Intensities increased 9/5 at 1667) | | | | | | distance |
| (A) | 17 17 32 | −35 43·8 | | | | −12·0 | 27E | 0·8 | — | 1·8 | 1665 | | | |
| | | | | | | −8·4 | 34E | | — | 3·2 | | | | 1·3(opt.) |
| | | | | | | −10·6 | 17E | 0·8 | — | 1·7 | 1667 | | | |
| (B) | 17 16 34 | −35 55·4 | | | | −9·5 | 19E | 0·8 | — | 3·7 | 1665 | | | |
| | | | | | | −6·2 | 25E | | — | 3·7 | | | | |
| | | | | | | −13·0 | 10E | 0·8 | — | Wide | 1667 | | | |
| | | | | | | −9·3 | 49E | | — | 2·5 | | | | |
| NGC 6357 | 17 22 19 | −34 17·5 | 353·2 | +0·67 | 76 | −5·8 | 4·8A | 1·4 | 0·06 | 2·8 | 1665 | −2 | −112 to | 0·6 |
| | | | | | | +5·3 | 2·4A | | 0·03 | 2·2 | | | +63E, | 1·3(opt.) |
| | | | | | | −10·9 | 2·4E | 1·4 | — | 2·0 | 1665 | | −21 to | |
| | | | | | | +0·7 | 3·7E | | — | 2·0 | | | 14A | |
| Sgr A (viii) | 17 42 30 | −28 58·7 | 359·95 | −0·045 | 260 | −138 | 39A | (0·4) | 0·15 | ~70 | 1667 | Nil | Same | 8–9 |
| | | | | | | −126 | 40A | | 0·15 | | | | features | |
| | See Section IV(viii) for references | | | | | −47 | 22A | | 0·08 | | | | | 6·5 |
| | | | | | | 0 | 48A | | 0·18 | ~70 | | | | ? local |
| | | | | | | +38 | 79A | | 0·31 | | | | | ~10 |
| | | | | | | +50 | 74A | | 0·29 | | | | | |
| Sgr B2 (ix) | 17 44 12 | −28 22·1 | 0·7 | −0·03 | 44 | See Section IV(ix) for reference | | | | | | | | |
| | | | 0°41′·2 | −0°2′·4 | | +61 | 6·8E | 0·8 | — | 2·7 | | | | |
| | | | 0°40′·0 | −0°2′·2 | | +67·5 | 47·6E | | — | 2·4 | 1665 | | | ~10 |
| | | | 0°39′·8 | −0°1′·8 | | +74 | 13·6E | | — | 6·0 | | +74 | | |
| | | | 0°40′·0 | −0°1′·8 | | +64 | 8·2A | | 0·19 | 2·6 | | | | |
| M 17 | 18 17 28 | −16 12·1 | 15·0 | −0·0 | 330 | +20 | 4·4A | (0·3) | 0·013 | (18) | 1667 | +20 | −40 to | 1·8(opt.) |
| | | | | | | | | | | | | | +110E, | |
| | | | | | | | | | | | | | −35 to | |
| | | | | | | | | | | | | | +90A | |
| W 49 (x) | 19 07 51 | +09 02·6 | 43·2 | +0·02 | 34 | +6·0 | E | | | | Each: | +7 | −80 to | ~13·5 |
| | | | | | | +13·0 | | | | | 1612, | | +100E, | |
| | See Section IV(x) for references | | | | | +16·3 | | | | | 1665, | | −10 to | |
| | | | | | | +18·1 | | | | | 1667, | | +70A | |
| | | | | | | +21·5 | | | | | 1720. | | | |

## II. Methods of Observation

The beamwidth of the 210 ft paraboloid is $12' \cdot 2$ arc at 1665 MHz; the frequency bandwidths in use were 10 and 37 kHz on the multichannel line receiver. Full details of the equipment, the calibrations, and the methods of observation have been given in a companion paper by Gardner, McGee, and Robinson (1967).

## III. The OH-line Sources

Twenty-eight thermal radio sources were investigated. OH was clearly detected in the direction of 24; probable detection (in that the line intensity was of the same order as the noise) was made for three; in one case no signal was seen above the sensitivity limit of the observation. Of two non-thermal sources, one (1548−56) gave a positive and the other (the Crab nebula) a negative result. The list of sources, their positions, and physical characteristics are presented in Table 1.

Column 1 of the table gives the name of the radio sources observed for OH. RCW numbers refer to the HII catalogue of Rodgers, Campbell, and Whiteoak (1960). The coordinate numbering system similar to that in the Parkes Catalogue of Radio Sources (Bolton, Gardner, and Mackey 1964) is used for optically unidentified or uncatalogued sources.

The second and third columns contain the source positions in celestial and galactic coordinates. The position of the maximum continuum intensity is usually given but in some cases, where well-resolved sources were partially mapped, the positions of maximum OH-line radiation are also included.

Aerial temperatures $T_c$ of the radio continuum sources at 1666 MHz are in column 4.

The details of the line observations are given in columns 5, 6, and 7; the radial velocity (referred to the local standard of rest) of a line feature, its intensity in aerial temperature $T_L$, and the equivalent r.m.s. noise level are included. The letters A and E refer to absorption and emission respectively. Values in parentheses mean that measurements were made only at 37 kHz resolution. The apparent opacity (the ratio of line to continuum intensities) for the absorption features is given in column 8. Columns 9, 10, 11, and 12 contain, respectively, the half-width of each feature (in km/sec), the line frequency of the observation, the radial velocity of excited hydrogen lines for the 13 sources, where they are available, and data on neutral hydrogen profiles.

An estimate of the distance from the Sun of each OH feature is made in the final column (from Section VI).

Ten sources in the table for which observations were more detailed are discussed in the following section. These same sources were observed for circular and linear polarization. The results are shown in Table 2. The basic observations of the circularly polarized intensities $I_{RH}$ and $I_{LH}$ (in relative units) are included with the corresponding radial velocities. The column headed $r$ is the degree of circular polarization. For linear polarization the degree of polarization $p$ and the position angle $\chi$ are given, together with estimated errors.

## IV. Detailed Observations for 10 Sources

### (i) *Crab Nebula*

Observations at line frequencies 1665, 1667, and 1720 MHz were made at the position of the maximum of the continuum intensity. No OH-line radiation was observed either in absorption or emission. The range at 10 kHz resolution was

Table 2

POLARIZATION MEASUREMENTS OF OH-LINE EMISSION

| Source | | Rad. Vel. (km/sec) | Circular Polarization $I_{RH}$ | $I_{LH}$ | $r$ | Sense | Linear Polarization $p$ | $\chi$ (deg) |
|---|---|---|---|---|---|---|---|---|
| Orion nebula | | +7·4 | 20 | 29 | 0·18 | LH | No measurements | |
| | | +19·5 | 19 | 23 | 0·10 | LH | | |
| RCW 38 | | | Limited obs. | | 0 | | <0·12 | |
| 1308−62 | | −39·2 | 28 | 0 | 1·0 | RH | 0·29±0·20 | 135±25 |
| | | −37·5 | 38 | 10 | 0·58 | RH | 0·45±0·12 | 171±15 |
| | | −30·5 | 55 | 15 | 0·57 | RH | 0·17±0·08 | 0±15 |
| | | −34·1 | 42 | 0 | 1·0 | RH | 0±0·10 | — |
| | | −32·4 | 19 | 3 | 0·73 | RH | 0·40±0·20 | 30±25 |
| 1608−51 | | −92·0 | 54 | 30 | 0·29 | RH | | |
| | | −90·3 | 49 | 30 | 0·24 | RH | 0·04±0·02 | 168±20 |
| | | −88·6 | 22 | 24 | 0·05 | LH | | |
| | | −86·9 | 14 | 2 | 0·80 | RH | | |
| 1617−50 | | −54·8 | 8 | 14 | 0·27 | LH | | |
| [161706 | | −51·2 | 44 | 34 | 0·13 | RH | | |
| −50 31·8] | | −46·5 | 12 | 18 | 0·09 | RH | | |
| | | −42·5 | 1 | 18 | 0·95 | LH | | |
| [161741 | | −54·3 | 0 | 11 | 1·0 | RH | | |
| −50 28·8] | | −51·2 | 44 | 34 | 0·13 | RH | 0·04±0·02 | 0 |
| | | −41·0 | 1 | 9 | 0·80 | LH | | |
| | | −49·9 | — | — | — | — | 0·06±0·02 | 25 |
| NGC 6334* | A | −12·2 | | | 0·82±0·20 | LH | | |
| | | −11·8 | | | — | | 0·07±0·04 | 120±20 |
| | | −10·1 | | | — | | 0·10±0·03 | 90±15 |
| | | −8·4 | | | 0·55±0·15 | RH | 0·04±0·02 | 75±20 |
| | B | −11·0 | | | 0·36±0·12 | LH | | |
| | | −9·5 | | | 0·02±0·06 | LH | No measurements | |
| | | −6·2 | | | 0·06±0·04 | RH | | |
| Sgr B2 | | +68 | Observed at one | | | LHC | | |
| | | +74 | circular | | | RHC | No measurements | |
| | | +77 | polarization only | | | RHC | | |
| W 49 | | +5·0 | | | | LHC | | |
| | | +13·0 | Observed at one | | | LHC | | |
| | | +16·4 | circular | | | RHC | No measurements | |
| | | +18·1 | polarization only | | | LHC | | |
| | | +21·5 | | | | LHC | | |

* See Gardner, McGee, and Robinson (1967)—summary here only.

0 to +22 km/sec in radial velocity. The observations were largely limited by instrumental effects; Goss (personal communication 1966) has found absorption for 1667 MHz with opacity of 0·005 at a velocity of +14 km/sec.

Observations at 21 cm (by R.X.M.) with 10 kHz bandwidth show strong HI absorption features at +4 and +11 km/sec with $\tau_H$ near unity.

(ii) *Orion Nebula*

The presence of wideband emission at 1665 MHz over the range —16 to +36 km/sec makes the Orion nebula unique among the 30 sources. The feature has been verified by 16 separate sets of profiles at 1665 MHz observed in September 1965 and February 1966. Its central frequency is at +8 km/sec.

Neutral hydrogen measurements were made (by R.X.M.) with similar equipment. The "expected" profile peak intensity occurred at +8·5 km/sec radial velocity. The overall line width —18 to +41 km/sec approximated to that of the OH feature. The absorption was unresolved at 10 kHz bandwidth. The maximum, $\tau = 1 \cdot 0$, was at radial velocity +2·5 km/sec. (Clark (1965) distinguished features at +2·5 and +4·5 km/sec.)

Circular polarization of the OH line is just measurable in two of the narrow peaks.

(iii) *RCW 38*

Line intensity ratios for the absorption at +1·3 km/sec are close to those given previously (McGee *et al.* 1965); 2·2 : 2·8 : 1 for 1665, 1667, and 1720 MHz respectively. No observations were taken at 1612 MHz. The positions of the continuum maximum and the maximum OH absorption are coincident.

Observations indicate OH-line emission of intensity 3·4°K at —9 km/sec at 1665 MHz, and 1·8°K at —8·5 km/sec at 1667 MHz.

(iv) *1308—62*

Observations were initially directed towards RCW 74. However, the radio continuum maximum was found about 14′ arc away at $13^{h}08^{m}38^{s}$, —62°20′·1 (1950·0). Appreciable emission at the 1665 MHz line was detected over a band of radial velocities —43 to —34 km/sec at points east of the above position. The results of position-finding observations are consistent with two point sources of line emission 5′ arc apart; one with radial velocity —35 km/sec at $13^{h}09^{m}58^{s}$, —62°21′·6, and the other with radial velocity —40 km/sec at $13^{h}09^{m}18^{s}$, —62°23′·1.

Dr. B. E. Westerlund of Mount Stromlo Observatory has kindly supplied us with prints of an Uppsala–Schmidt plate centred on RCW 74. No HII region is visible either at the position of the continuum maximum or that of the OH-line source.

This is some support for a distance of either 8·5 or 3 kpc derived from the kinematic model. We believe that the distance of 3 kpc, on the outside edge of the Sagittarius arm, is the more likely. The OH sources would then be 4·5 pc apart. The separation of the OH emitters from the position of the continuum maximum would be 10 and 3·5 pc at —35 and —40 km/sec respectively. The significance of the separation of the continuum and OH emission peak positions is complicated by the complexity of the continuum source itself. Its apparent peak position depends on angular resolution.

No significant amount of OH absorption was observed at 1665 MHz but opacities up to 0·1 occur for the 1667 line over the band of radial velocities from —46 to —37 km/sec near the position of peak emission at 1665 MHz.

(v) *1608−51*

Position finding was used to locate the maximum of the 1665 MHz line emission at $16^{h}08^{m}39^{s}$, $-51°21'\cdot3$ (1950·0) or approximately $3'\cdot5$ away from the continuum maximum at $16^{h}08^{m}14^{s}$, $-51°18'\cdot4$ (1950·0). This separation is 11 pc for a distance of 10·5 kpc.

The maximum values of the absorption features near −99 km/sec were observed at the position of the continuum source.

One set of observations was made at 1667 MHz at $16^{h}08^{m}14^{s}$, $-51°19\cdot1$ (1950·0). The absorption features near −99 km/sec were approximately equal to those at 1665 MHz but an emission feature near −91 km/sec was 2·5 times weaker.

(vi) *1617−50*

The maximum of the 1665 MHz line emission was found at $16^{h}17^{m}16^{s}$, $-50°27'\cdot6$ (1950·0), and angular distance of $3'\cdot9$ from the continuum maximum $16^{h}17^{m}06^{s}$, $-50°31'\cdot0$ (1950·0). For a distance of 4 kpc the separation is 4·5 pc.

The line profile displayed absorption dips at −58, −48, and −45 km/sec and two peaks of emission at −55 and −52 km/sec. It is possible that the true absorption may be masked to some extent by the emission features.

A check observation was taken in one position ($16^{h}17^{m}41^{s}$, $-50°28'\cdot8$) at 1667 MHz. Absorption dips at the same radial velocities and of similar intensity to those at 1665 MHz were present. Emission lines were scarcely above noise.

(vii) *NGC 6334*

The HII region which is relatively close to the Sun (1·3 kpc) has been discussed in considerable detail by Gardner, McGee, and Robinson (1967).

In this case two sources of OH-line emission are separated from each other by $16'\cdot5$ arc or $\sim$ 6 pc. They are situated along a line of galactic latitude and spaced approximately equally either side of the continuum maximum. The OH absorption is centred on the continuum maximum.

(viii) *Sagittarius A*

The entry in Table 1 merely gives some of the important features of the absorption profile, which has been discussed elsewhere (e.g. Goldstein *et al.* 1964; Robinson *et al.* 1964).

(ix) *Sagittarius B2*

Observations at 10 kHz resolution were confined to a band covering the radial velocity range +60 to +80 km/sec approximately. OH emission was observed on all four lines (1612, 1665, 1667, and 1720 MHz). The profiles have been given by McGee *et al.* (1965).

Position finding located the maximum 1665 MHz line emission at $l^{\mathrm{II}} = 0°40'$, $b^{\mathrm{II}} = -0°2'\cdot2$, which is coincident with the position of the thermal source observed at 6 cm wavelength by Broten *et al.* (1965) and that of the more northerly component of a double source observed at 10 cm by Cooper and Price (1964). At 18 cm the components are unresolved and the continuum maximum appears displaced in longitude from the OH position.

(x) *W 49*

Results of observations at higher angular and/or frequency resolutions are available (e.g. Palmer and Zuckerman 1966; Rogers *et al.* 1967).

Continuum observations at 18 cm (by F.F.G.) have shown that the source is a double; one component is well away from the line emission source at $19^h 08^m 50^s$, $+09°02'\cdot0$ (1950·0) and the other at $19^h 07^m 57^s$, $+09°01'\cdot8$ (1950·0).

We find the OH-line emission at $19^h 07^m 42^s$, $+09°01'\cdot3$ for radial velocities $+6\cdot0$ and $+21\cdot5$ km/sec and $19^h 07^m 50^s$, $+09°01'\cdot3$ for radial velocities $+13\cdot0$, $+16\cdot3$, and $+18\cdot1$ km/sec. These are approximately 2′ west of the corresponding two positions found by interferometry by Rogers *et al.* (1967).

At a distance of 13·5 kpc the OH sources are 6 pc apart and about 10 pc from the continuum source.

## V. Discussion of Results

### (*a*) *Absorption Lines*

OH absorption has been detected in the directions of 26 of the 30 sources. No absorption was seen in the directions of the Crab nebula, 30 Doradus, the Orion nebula (already seen to have peculiar emission), and W 49. However, in the last case it is possible that the intense emission may mask weak absorption. The great majority of the present sources exhibit absorption at two or more radial velocities.

It should be borne in mind that the present sources were selected on the basis of the strength of their thermal radiation. Other types of radio sources should be investigated before we can draw conclusions about the galactic distribution of OH.

### (*b*) *Opacities*

The apparent opacities range from 0·4 to less than 0·002. There are now enough data for a comparison of the opacities for OH and neutral hydrogen in several positions in the galaxy. Six of the OH measurements can be compared directly with the H-line absorption results obtained by Clark (1965). The ratios of opacities $\tau_{\mathrm{OH}}/\tau_{\mathrm{H}}$ are listed in Table 3. Where line widths were measured in both cases the ratios $(\sigma\tau)_{\mathrm{OH}}/(\sigma\tau)_{\mathrm{H}}$ are included; this ratio is directly proportional to $(N_{\mathrm{OH}}/N_{\mathrm{H}})\cdot(T_{\mathrm{H}}/T_{\mathrm{OH}})$. Here $\sigma$ is the dispersion in kilohertz when a Gaussian shape is assumed, $N_i$ the surface density of molecules or atoms, and $T_i$ the relevant excitation temperature.

It can be seen in the table that, although the greatest ratio of $\tau_{\mathrm{OH}}$ to $\tau_{\mathrm{H}}$ is in the +40 km/sec component of Sagittarius A, there is no systematic variation in the ratio with distance from the centre, as suggested by the early observations of Sagittarius A and Cassiopeia A (Robinson *et al.* 1964).

### (*c*) *Emission Lines*

OH emission lines were observed at 1665 MHz in 14 of the sources. There was no obvious correlation of OH emission with the intensity of the continuum. Some intense HII regions, such as RCW 38 ($T_{\mathrm{c}} = 115°$K) and $\eta$-Carinae ($T_{\mathrm{c}} = 110°$K), produced no emission at this frequency, while the relatively weak RCW 36 ($T_{\mathrm{c}} = 17°$K) produced 5·4°K of anomalous OH-line emission.

TABLE 3

COMPARISON OF THE OPACITIES OF OH AND HI

| Source | OH | | | | HI | | | | $\tau_{OH}/\tau_H$ | $\sigma\tau_{OH}/\sigma\tau_H$ |
|---|---|---|---|---|---|---|---|---|---|---|
| | Rad. Vel. (km/sec) | $\tau_{OH}$ | $\sigma$ (kHz) | $\sigma\tau_{OH}$ | Rad. Vel. (km/sec) | $\tau_H$ | $\sigma$ (kHz) | $\sigma\tau_H$ | | |
| Crab nebula | — | $<0\cdot002$ | — | | +11 | 0·9 | 6·0 | 5·4 | $<0\cdot002$ | — |
| RCW 38 | +2·9 | 0·10 | 15·3 | 1·53 | +3·8 | 2 | 12·6 | $>25\cdot2$ | $<0\cdot05$ | $<0\cdot06$ |
| NGC 6334 | +5·5 | 0·05 | 8·3 | 0·42 | +4·2 | 0·6 | 22 | 13·2 | 0·08 | 0·03 |
| | −4·5 | 0·10 | 10·1 | 1·01 | −5·7 | 1·5 | 6·9 | 10·4 | 0·07 | 0·10 |
| NGC 6357 | +5·3 | 0·03 | 5·2 | 0·16 | +4·9 | $>1\cdot4$ | 5·4 | $>7\cdot6$ | $<0\cdot02$ | $<0\cdot02$ |
| Sgr A | −47 | 0·08 | 75(est.) | $\sim6\cdot0$ | −54 | 1·1 | 13·7? | 15·1 | 0·07 | 0·40 |
| | 0 | 0·18 | 75(est.) | $\sim13\cdot5$ | 0 | $>3$ | $<45$ | 135 | 0·06 | 0·10 |
| * | +40 | 0·9 | 128 | | +40 | $\leqslant2$ | | | $>4\cdot5$ | |
| M 17 | +20 | 0·013 | 42·5 | 0·55 | +21 | 1·6 | 10·5 | 16·8 | | 0·03 |
| Cas A * | −0·8 | 0·016 | 5·5 | | −0·8 | 2·0 | | | 0·008 | |
| * | +48·2 | 0·016 | 10·7 | | +48·2 | 3·4 | | | 0·0047 | |

* From Robinson *et al.* (1964).

### (*d*) *Line Half-widths*

From the absorption lines observed with 10 kHz filters, for 31 cases of apparently simple features, the mean half-width is $3 \cdot 1 \pm 1 \cdot 2$ (s.d.) km/sec, or $2 \cdot 5$ km/sec when corrected for the instrumental bandwidth (equivalent to $1 \cdot 7$ km/sec).

For 21 simple cases of emission, as seen with 10 kHz resolution, the mean width is $2 \cdot 7 \pm 0 \cdot 8$ (s.d.) km/sec, or $2 \cdot 0$ km/sec corrected.

### (*e*) *The Relative Positions of OH with Respect to the Thermal Sources*

In Section IV the positions of the radio continuum maxima and the positions of maximum OH emission and absorption were discussed for a number of individual sources. In many cases of emission lines the OH maximum was found to be displaced from the 18 cm continuum maximum. (The angular distances are given in Section IV and amount to several parsecs for the distances assumed.) For the few cases that have been investigated, the OH absorption maximizes at the same position as the continuum.

For three cases of double OH emission maxima the component separation was a few minutes of arc (equivalent to 2–10 pc at the estimated source distances).

### (*f*) *Radial Velocities of OH and Recombination H Lines*

Fifteen comparisons may be made in Table 1 between the radial velocities of OH-line components (six in emission and nine in absorption) and those of the 126 $\alpha$ H-line observed at 3249 MHz by McGee and Gardner (1967). The 126 $\alpha$ lines are quite wide, $\sim$ 32 km/sec half-width. The average difference between the 126 $\alpha$ velocity and that of the nearest OH feature is $\sim$ 2 km/sec, which is about equal to the measurement errors of the 126 $\alpha$ peaks. Since the recombination lines are generated in the HII regions themselves, the above comparison supports the idea that the OH emission and some of the absorption frequently occur close to the HII region.

### (*g*) *Radial Velocities of OH and HI Lines*

It can be seen in Table 3 that good agreement exists between the velocities of OH and HI absorption line components. The neutral hydrogen values in Table 1 are comparatively few in number and cover large ranges of velocity. The general impression gained is that considerable quantities of OH gas are spread throughout the neutral hydrogen clouds in spiral arms.

### (*h*) *Polarization*

The polarization data for the OH emission (Table 2) should be regarded as being of a preliminary nature. The bandwidth of 10 kHz smooths the polarization components, many of which are known to have half-widths of less than 1 kHz. However, the degree of circular polarization $r$ approaches 1 for many components. The sense changes from component to component but no recognizable pattern has been detected in any of the profiles studied.

No polarization was found in the strong absorption lines from RCW 38, the two absorption components in NGC 6334, or the wide absorptions in Sagittarius B2 and Sagittarius A.

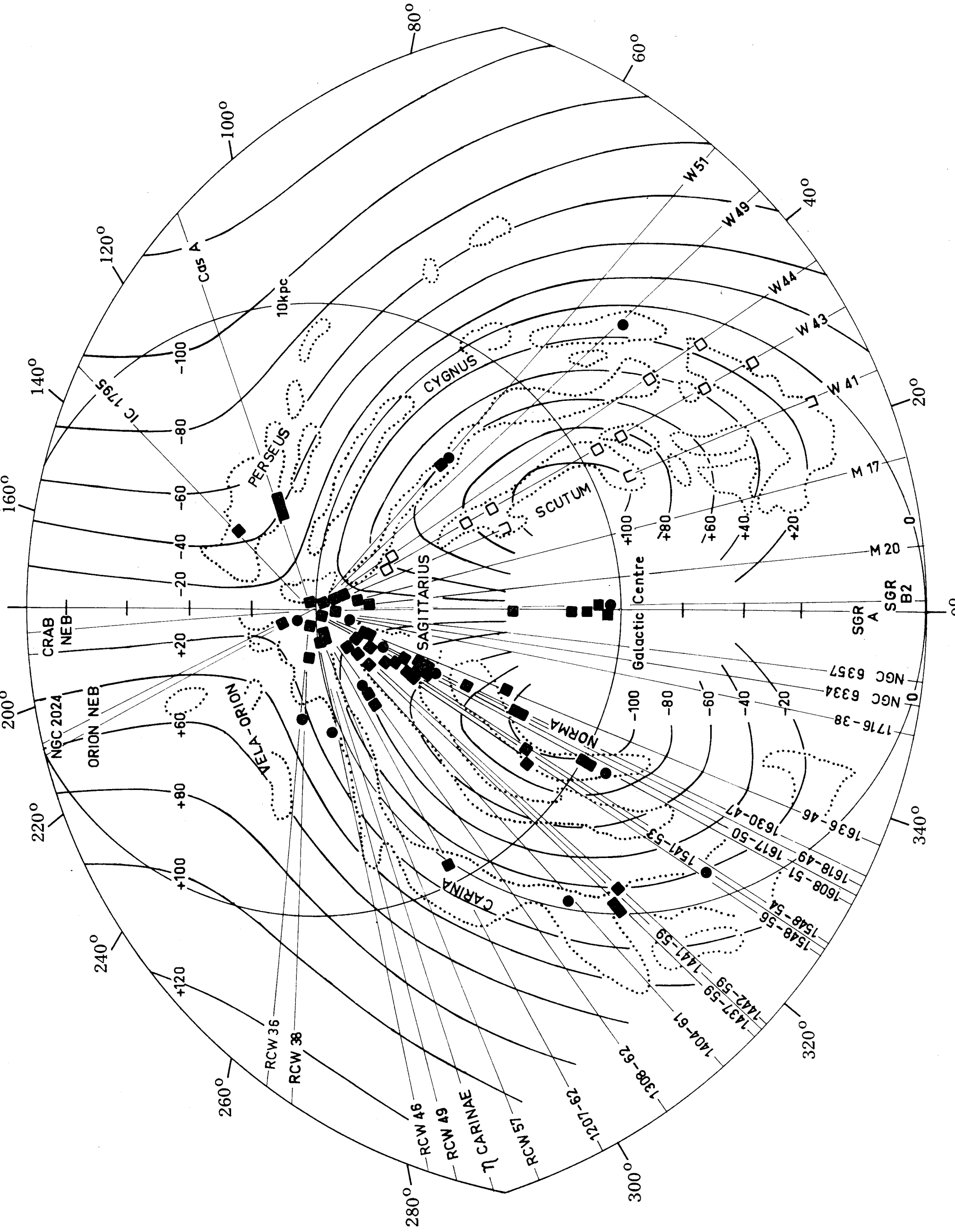

0°
20°
40°
60°
80°
100°
120°
140°
160°
180°
200°
220°
240°
260°
280°
300°
320°
340°
10kpc
Cas A
IC 1795
PERSEUS
CYGNUS
SCUTUM
SAGITTARIUS
Galactic Centre
NORMA
CARINA
VELA-ORION
CRAB NEB
NGC 2024
ORION NEB
W51
W49
W44
W43
W 41
M 17
M 20
SGR B2
SGR A
NGC 6357
NGC 6334
1716-38
1636-46
1630-47
1617-50
1618-49
1608-51
1548-54
1548-56
1541-53
1441-59
1442-59
1437-59
1404-61
1308-62
1207-62
RCW 57
η CARINAE
RCW 49
RCW 46
RCW 38
RCW 36


Fig. 1

In general the degree of linear polarization was low. The highest value, $p = 0{\cdot}45$, was observed in 1308−62. In this source the sense of the circular polarization was right-handed over all components.

## VI. Location of OH Clouds

Each feature listed in Table 1 is believed to represent a "cloud" of OH gas, each with its own peculiar radial velocity. In almost every case the velocity is compatible with differential galactic rotation, and thus we may use a kinematic model to locate the clouds. Figure 1 shows an attempt to do this.

The diagram shows (1) contours of radial velocity in the galactic plane derived from the circular orbit model of galactic rotation, "northern hemisphere", discussed by, for example, Kerr and Westerhout (1965); (2) dotted outlines, representing the distribution of neutral hydrogen as positioned by the same model; (3) catalogue numbers and longitude lines of the radio continuum sources.

When the radial velocity and direction of a cloud place it inside the circle of zero velocity of the model, ambiguity of position exists and some additional information must be used to resolve the ambiguity. In several cases optical distances to HII regions have been estimated independently. Again, if an HII region has been photographed and catalogued it is probably within a few kiloparsecs of the Sun. Further, it is plausible to regard the continuum sources of larger angular size as being nearer. Finally, absorption would be expected to occur between the HII region and the Sun, while, as shown in the preceding section, OH emission usually emanates from points in the vicinity of HII regions. The order of positioning emission and absorption features gives a clue to locality. Source 1608−51 is such an example. We have placed the OH clouds at the larger distances because then the emission cloud is beyond the two absorbing clouds. In addition, a study of neutral hydrogen line profiles in the same direction can give an indication of which is the most likely position.

Having decided on cloud positions by one or more of the above methods it appears that with the exception of the galactic nucleus source, Sagittarius A, all the sources with higher aerial temperature lie within 2 kpc of the Sun.

In Figure 1 the locations of the emission line clouds are shown by full circles and the locations of the absorbing clouds by squares. Distances to the nearest half kiloparsec are listed in the final column of Table 1. In addition to that for the 30 sources, radial velocity information was extracted for 8 more sources observed elsewhere (Robinson and McGee 1967).

It must be concluded from Figure 1 that many clouds of OH gas are dispersed through the main spiral arms of neutral hydrogen as well as through those associated in some way with HII regions.

---

Fig. 1.—The position of OH clouds projected onto the galactic plane. The squares represent absorption components, the circles, emission components. Contours of radial velocity derived from the circular orbit model of galactic rotation are included. (Dotted outlines represent the distribution of neutral hydrogen.) The catalogue number and direction of each continuum source are marked. The open squares and brackets represent possible positions taken from profiles observed elsewhere. The Sun–galactic centre distance is 10 kpc.

## VII. Conclusion

The preliminary survey of galactic sources shows that OH gas may be detected in absorption in the directions of most radio sources near the galactic plane.

Although the sample available was fairly small, it appears that the ratio of OH to HI is less in the outer arms and is much increased near the galactic nucleus. However, the ratio varies somewhat randomly in the inner arms (Carina, Cygnus, Sagittarius, and Norma–Scutum) rather than displaying a progressive increase towards the centre.

The comparison of radial velocities of OH and recombination H lines leaves little doubt that both emitting and absorbing clouds frequently occur near HII regions.

Polarization measurements of the stronger sources indicate high degrees of circular and low degrees of linear polarization.

The work has underlined the need for more OH measurements at increased frequency resolution and sensitivity. Combination of these data with data from H-line absorption and excited hydrogen emission should add greatly to our knowledge of the interstellar medium.

## VIII. References

Bolton, J. G., Gardner, F. F., and Mackey, M. B. (1964).—*Aust. J. Phys.* **17**, 340–72.

Broten, N. W., Cooper, B. F. C., Gardner, F. F., Minnett, H. C., Price, R. M., Tonking, F. G., and Yabsley, D. E. (1965).—*Aust. J. Phys.* **18**, 85–90.

Clark, B. G. (1965).—*Astrophys. J.* **142**, 1398–422.

Cooper, B. F. C., and Price, R. M. (1964).—Symp. IAU–URSI No. 20 (Canberra 1963). pp. 168–72.

Dieter, N. H., Weaver, H., and Williams, D. R. W. (1966).—*Sky Telesc.* **31**, 132–6.

Gardner, F. F., McGee, R. X., and Robinson, B. J. (1967).—*Aust. J. Phys.* **20**, 309–24.

Goldstein, S. J., Gundermann, E. J., Penzias, A. A., and Lilley, A. E. (1964).—*Nature, Lond.* **203**, 65–6.

Kerr, F. J., and Westerhout, G. (1965).—*In* "Stars and Stellar Systems". (Eds. A. Blaauw and M. Schmidt.) Vol. 5, pp. 167–202. (Univ. Chicago Press.)

McGee, R. X., and Gardner, F. F. (1967).—*Nature, Lond.* **213**, 579.

McGee, R. X., Robinson, B. J., Gardner, F. F., and Bolton, J. G. (1965).—*Nature, Lond.* **208**, 1193–5.

Palmer, P., and Zuckerman, B. (1966).—Harvard Radio Astron. Reprint HRAP 124.

Robinson, B. J. (1967).—"Radio Astronomy and the Galactic System." (Ed. H. van Woerden.) (Academic Press: London.) (In press.)

Robinson, B. J., Gardner, F. F., van Damme, K. J., and Bolton, J. G. (1964).—*Nature, Lond.* **202**, 989–91.

Robinson, B. J., and McGee, R. X. (1967).—OH molecules in the interstellar medium. *A. Rev. Astr. Astrophys.* **5** (in press).

Rodgers, A. W., Campbell, C. T., and Whiteoak, J. B. (1960).—*Mon. Not. R. astr. Soc.* **120**, 1–8.

Rogers, A. E. E., Moran, J. M., Crowther, P. P., Burke, B. F., Meeks, M. L., Ball, J. A., and Hyde, G. M. (1967).—*Astrophys, J.* **147**, 369–77.